

## Formation of Multinary Intermetallics from Reduction of Perovskites by Aluminum Flux: $M_3Au_{6+x}Al_{26}Ti$ ( $M = Ca, Sr, Yb$ ), a Stuffed Variant of the $BaHg_{11}$ Type

Susan E. Latturmer and Mercuri G. Kanatzidis\*

Department of Chemistry, Michigan State University, East Lansing, Michigan 48824

Received August 14, 2003

New intermetallic phases were synthesized by reacting oxidic perovskites and gold metal in aluminum flux. The combination of  $MTiO_3$  ( $M = Ca, Sr, Ba$ ) and Au metal in excess molten aluminum produces quaternary compounds  $M_3Au_{6+x}Al_{26}Ti$  with a stuffed  $BaHg_{11}$  structure type. An analogue with  $M = Yb$  was also synthesized; it shows mixed valent behavior.

The thermite reaction is a well-known and memorable demonstration of the utility of the reducing ability of aluminum to convert  $Fe_2O_3$  to molten iron. Preliminary investigations have been carried out on the aluminothermic synthesis of simple borides such as  $AlB_{12}$  and  $LaB_6$  via reduction of  $B_2O_3$ .<sup>1</sup> The efficacy of aluminum in the reduction of rare earth oxides has been demonstrated in the formation of complex intermetallics such as  $Sm_2Ni(Ni_xSi_{1-x})Al_4Si_6$  from the combination of  $Sm_2O_3$ , Ni, and Si in aluminum flux.<sup>2</sup> Less work has been done in exploring the use of aluminum as a reducing agent for more complex oxides, however. In the results described here, perovskites  $MTiO_3$  ( $M = Ca, Sr, Ba$ ) placed in molten aluminum react to form intermetallic phases. In the presence of gold, cubic  $BaHg_{11}$  variant phases  $M_3Au_{6+x}Al_{26}Ti$  are produced.

The impetus for this investigation was the isolation of  $Yb_3Au_7Al_{26}Ti$  from an aluminum flux reaction intended to produce  $YbAu_3Al_7$ .<sup>3</sup> In addition to this ternary phase, a number of crystals of a cubic phase were isolated. The crystallographic analysis indicated the structure of these crystals was a variant of the  $BaHg_{11}$  type.<sup>4</sup> The identity of the atom in the 1b Wyckoff site was unclear; the electron density at this location was too high for aluminum, and not

high enough for gold or ytterbium. Careful elemental analysis indicated the presence of a very small amount of Ti in the crystals. The aluminum flux had reduced some unannealed titania cement (a mixture of complex oxides) in the crucible, allowing metallic titanium to be incorporated into the product.<sup>5</sup> It was therefore decided to investigate this reducing behavior further by using complex oxides (perovskites) as reactants.

Perovskites of the type  $MTiO_3$  were combined with gold and excess aluminum metal as a reactive, reducing flux in a 1:2:20  $MTiO_3/Au/Al$  ratio.  $M_3Au_{6+x}Al_{26}Ti$  grows from the flux as large, faceted spheroid chunks. Also formed in the reaction are binary intermetallics such as  $TiAl_3$  and  $BaAl_4$ , recrystallized gold, and oxide powder. The yield of  $M_3Au_{6+x}Al_{26}Ti$  is fairly low (ca. 10%); higher yields of around 50% based on the amount of gold used are obtained by using elemental reactants instead of perovskite precursors. The material is fairly stable to 5 M NaOH solution but dissolves in acids.

While the structure of  $Ba_3Au_7Al_{26}Ti$  has not been solved yet, the structure of  $M_3Au_{6+x}Al_{26}Ti$  ( $M = Yb, Ca, Sr$ ) is closely related to that of  $BaHg_{11}$ , as shown in Figure 1.<sup>6</sup> These compounds form in cubic space group  $Pm\bar{3}m$ , featuring a unit cell centered by titanium coordinated by a cuboctahedron of neighboring aluminum sites. An early transition metal atom (such as Ti) surrounded by a cuboctahedron of 12 Al atoms is a common structural motif in early transition metal aluminides such as  $TiAl_3$  and  $ZrAl_3$ .<sup>4</sup> This suggests that the presence of Ti might template the formation of the cubic  $M_3Au_7Al_{26}Ti$  structure. Our work indicates that all early transition metals in groups 4–7 (from Ti to Re) can be incorporated into this site.

One difference between the  $BaHg_{11}$  and  $M_3Au_{6+x}Al_{26}Ti$  structures is the presence in the latter of an additional atomic

\* To whom correspondence should be addressed. E-mail: kanatzid@cem.msu.edu.

- (1) (a) Peshev, P. *J. Solid State Chem.* **1997**, *133*, 237–242. (b) Kirillova, N. V.; Kharlamov, A. I.; Loichenko, S. V. *Inorg. Mater.* **2000**, *36*, 776.
- (2) Chen, X. Z.; Sportouch, S.; Sieve, B.; Brazis, P.; Kannewurf, C. R.; Cowen, J. A.; Patschke, R.; Kanatzidis, M. G. *Chem. Mater.* **1998**, *10*, 3202–3211.
- (3) Latturmer, S. E.; Bilc, D.; Ireland, J. R.; Kannewurf, C. R.; Mahanti, S. D.; Kanatzidis, M. G. *J. Solid State Chem.* **2003**, *170*, 48.
- (4) Villars, P. *Pearson's Handbook: Crystallographic Data for Intermetallic Phases*; ASM International: Materials Park, OH, 1997.

(5) Purposely adding Ti as a reactant increased the yield of  $Yb_3Au_7Al_{26}Ti$ .

(6) XRD data for  $Sr_3Au_7Al_{26}Ti$  as a representative compound:  $Pm\bar{3}m$ ,  $a = 8.7367(6)$  Å;  $V = 666.87(8)$  Å<sup>3</sup>,  $Z = 1$ ,  $\rho = 6.165$  g/cm<sup>3</sup>. Total reflections: 10687; unique reflections, 383; index range  $-14 \leq h, k, l \leq 14$ .  $R1/wR2$  for  $I > 2\sigma(I)$ : 0.0237/0.0435; for all data, 0.0379/0.0465.

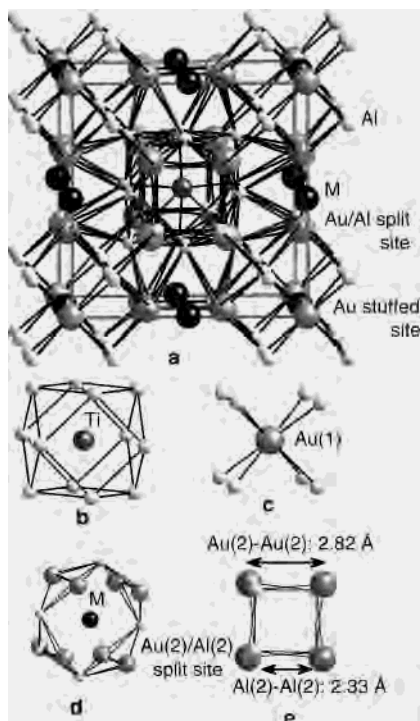


**Figure 1.** (a) The structure of  $M_3Au_{6+x}Al_{26}Ti$ , in the disordered  $Pm\bar{3}m$  subcell. (b) The titanium site, in a cuboctahedron of 12 Al(3) atoms. (c) The stuffed site within a cage of 8 Al atoms, occupied by Au(1). (d) The environment around the M atom includes Al(1) and the Al(2)/Au(2) split site. (e) The Al(2)/Au(2) split site rhombus.

**Table 1.** Occupation of the Stuffed Site of  $M_3Au_{6+x}Al_{26}Ti$

compd	unit cell edge (Å)	Au(1) occupancy $x$
$Yb_3Au_{6+x}Al_{26}Ti$	8.6509(6)	0.844(7)
$Sr_3Au_{6+x}Al_{26}Ti$	8.7367(6)	0.990(8)
$Ca_3Au_{6+x}Al_{26}Ti$	8.6631(5)	0.80(1)

position in the center of a cube of eight aluminum atoms. A gold atom occupies this site (the 1a Wyckoff site);  $M_3Au_{6+x}Al_{26}Ti$  can therefore be described as a stuffed variant of  $BaHg_{11}$ . The stuffing of the site in the compounds studied here varies from 80% to 100% (Table 1). It is possible that the size of the unit cell controls the filling of this site, with a larger unit cell (such as  $Sr_3Au_7Al_{26}Ti$ ) allowing room for full occupancy by gold. Gold-centered  $Al_8$  cubes are a feature of the antifluorite structure  $AuAl_2$  phase and have also been observed in multinary intermetallics such as  $Th_2Au_3Al_4Si_2$  and  $YbAu_4Al_8Si$ .<sup>7</sup>

Another variation from the parent structure is a splitting of the 12i Wyckoff site to allow for occupancy of this site by a mixture of Al and Au. A possible reason for this splitting is to allow the formation of suitable bond lengths between the aluminum or gold atoms and the neighboring M atom ( $M = Ca, Sr, Yb$ ). It also allows for Al–Au bonds of an appropriate length between adjacent split sites (see Figure 1). This produces an  $Au_2Al_2$  rhombus with strong Au–Al bonds (2.57–2.66 Å in length, similar to that found in bulk  $AuAl_2$ ) instead of  $Al_4$  or  $Au_4$  squares. The disorder in

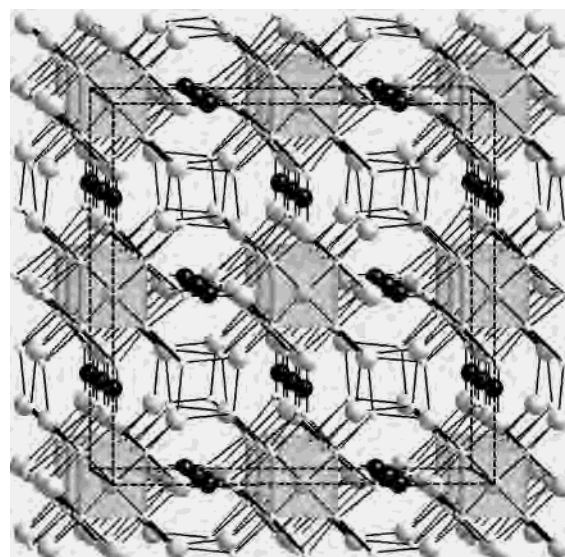


**Figure 2.** The  $Fm\bar{3}m$  cell with  $a^* = 2a$ ; the  $TiAl_{12}$  cuboctahedra have been removed to make the Au/Al rhombi visible. The light gray cubes are the  $Al_8$  cubes containing the stuffed site.

rhombus orientation resulting from this splitting is averaged over the crystal, resulting in  $Pm\bar{3}m$  symmetry.

These differences were also noted in a report of another stuffed  $BaHg_{11}$  variant.  $Y_3Ni_{6+x}Al_{26}Ta$  was formed when pellets of  $YNi_2Al_7$  were annealed in a Ta crucible. In this paper, the two potential supercells that could result from ordering of the orientation of the rhombi were briefly mentioned, although no evidence of ordering was observed.<sup>8</sup> One of these ordered supercells is depicted in Figure 2, a cubic  $Fm\bar{3}m$  cell with a cell edge double that of the  $Pm\bar{3}m$  subcell. The other possible supercell (not shown) is a rhombohedral cell ( $R\bar{3}m$ ) derived from the subcell by  $a^* = a\sqrt{2}$  and  $c^* = a\sqrt{3}$ . The  $M_3Au_{6+x}Al_{26}Ti$  ( $M = Yb, Sr$ ) compounds studied here did not show any signs of ordering in their X-ray diffraction data, but the calcium analogue did.

The single crystal XRD data for  $Ca_3Au_{6.8}Al_{26}Ti$  initially indexed as cubic  $F$  with an  $a = 17.3434(9)$  Å cell; the  $Fm\bar{3}m$  space group of the supercell was indicated. However, the structure could not be solved in this space group, even when the supercell model was put in as a starting point. Powder diffraction data for this compound is shown in Figure 3; data for  $Sr_3Au_7Al_{26}Ti$  and theoretical patterns for the disordered subcell and the ordered supercell are also shown for comparison. The X-ray powder pattern of  $Ca_3Au_7Al_{26}Ti$  does show the (113), (371), and (795) supercell reflections, but they are weak; other expected supercell reflections such as the (111) and (115) peaks are absent. An attempt was therefore made to solve the single crystal structure in the  $Pm\bar{3}m$  subcell. This proved successful, resulting in an R1 of 0.0357 despite the alarming necessity of ignoring the supercell data (number of unique reflections reduced from 704 to 364). Evidently, even within a “single” crystal of this compound there exist ordered domains and disordered domains. A number of single crystals were screened with similar results.

(7) (a) Latturmer, S. E.; Bilc, D.; Mahanti, S. D.; Kanatzidis, M. G. *Chem. Mater.* **2002**, *14*, 1695–1705. (b) Latturmer, S. E.; Bilc, D.; Mahanti, S. D.; Kanatzidis, M. G. *Chem. Commun.* **2003**, *18*, 2340–2341.

(8) Gladyshevskii, R. E.; Cenual, K. *J. Alloys Compd.* **1996**, *240*, 266.

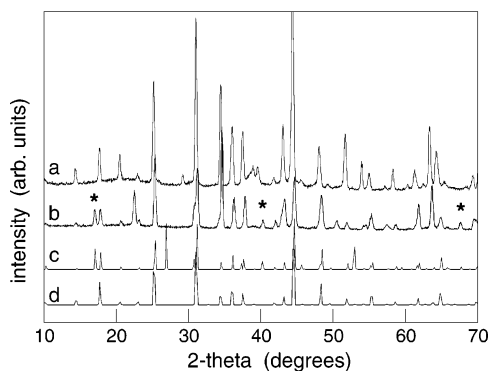


**Figure 3.** Powder X-ray diffraction data for  $\text{Sr}_3\text{Au}_{6.8}\text{Al}_{26}\text{Ti}$  (a) and  $\text{Ca}_3\text{Au}_7\text{Al}_{26}\text{Ti}$  (b), and calculated patterns for the  $Fm\bar{3}m$  supercell (c) and the  $Pm\bar{3}m$  subcell (d). The observed supercell reflections in the  $\text{Ca}_3\text{Au}_{6.8}\text{Al}_{26}\text{Ti}$  data are marked with asterisks.

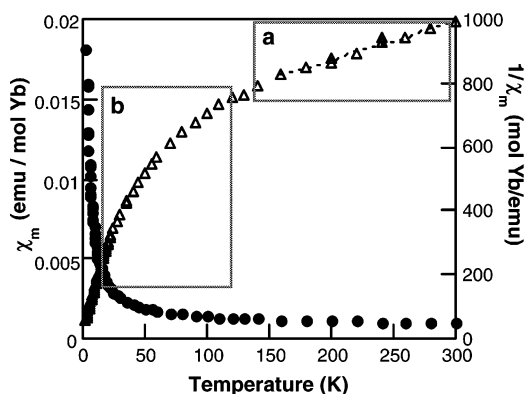


**Figure 4.** Magnetic susceptibility data for  $\text{Yb}_3\text{Au}_{6.8}\text{Al}_{26}\text{Ti}$ , showing the regions of inhomogeneous valence at high temperature (a), and fluctuating valence at low temperature (b).

Magnetic susceptibility measurements on the Ca and Sr containing analogues show Pauli paramagnetic behavior consistent with metallic samples containing no localized magnetic moments.  $\text{Yb}_3\text{Au}_7\text{Al}_{26}\text{Ti}$  shows more complex behavior, as seen in Figure 4. The inverse susceptibility data above 150 K is roughly linear and can be fit using the Curie–Weiss law. The fit to these points indicates a magnetic moment of  $0.86 \mu_B$  per Yb ion. This is well below the  $4.86 \mu_B$  expected for  $\text{Yb}^{3+}$  ions, but higher than should be observed for diamagnetic  $\text{Yb}^{2+}$  ions.<sup>9</sup>

Since there is only one crystallographic Yb site in the  $\text{Yb}_3\text{Au}_7\text{Al}_{26}\text{Ti}$  structure, this nonintegral valence cannot be attributed to a mixture of distinct  $\text{Yb}^{2+}$  and  $\text{Yb}^{3+}$  species (as in mixed valence compounds). Intermediate valence behavior is also unlikely, since the fluctuations in valence characteristic of this state (resulting from 4f-conduction electron interactions) usually vary with temperature.<sup>10</sup> The ytterbium valence in  $\text{Yb}_3\text{Au}_7\text{Al}_{26}\text{Ti}$  is fairly constant above 150 K. This leaves the possibility of inhomogeneous valence, which can occur in disordered compounds due to the variation in neighboring atoms around the paramagnetic site.

(9) Kittel, C. *Introduction to Solid State Physics*; John Wiley & Sons: New York, 1986.

(10) Varma, C. M. *Rev. Mod. Phys.* **1976**, *48*, 219.

As shown in Figure 1, the ytterbium site is closely coordinated to the Au(2)–Al(2) split site. The disorder in the occupancy and  $\text{Au}_2\text{Al}_2$  rhombi orientations in the structure can easily produce local inhomogeneities around the Yb sites in a bulk sample. Similar behavior was observed in  $\text{YbPd}_3\text{Ga}_8$ , a compound which is also described as a disordered variant of  $\text{BaHg}_{11}$ .<sup>11</sup>

As the  $\text{Yb}_3\text{Au}_7\text{Al}_{26}\text{Ti}$  sample is cooled below 150 K, the inverse susceptibility begins to show nonlinear behavior, indicating temperature-dependent valence behavior. This likely signals the onset of valence fluctuation. This is often observed in compounds with ytterbium f-bands near or at the Fermi level. As the temperature reaches a certain range, the energetics become favorable for these f-bands to begin to mix with the conduction bands of the sample. This results in a temperature-dependent intermediate valence state. Other ytterbium intermetallics with similar behavior include  $\text{YbAu}_3\text{Al}_7$  and  $\text{YbAu}_4\text{Al}_8\text{Si}$ .<sup>3,7b</sup>

In reducing perovskites to form complex intermetallic compounds, molten aluminum metal has proven to be an extremely useful synthetic medium in yet another way. Its reactivity toward highly stable multinary oxides introduces a new field of exploration, with a wide variety of compounds that can potentially be used as reactants in aluminum flux. Advantages of complex oxides as reactants include inherent premixing of elements and finely divided form, less loss of volatile reactants such as alkaline earths,<sup>12</sup> and lower price than elemental reagents.

Ongoing experiments indicate that the stuffed  $\text{BaHg}_{11}$  structure is a very common result when a late transition metal, an early transition metal, and a rare earth or alkaline earth metal are combined in aluminum flux. We have prepared a wide range of  $\text{M}_3\text{Au}_7\text{Al}_{26}\text{T}$  compounds (with  $\text{M} = \text{Ca}, \text{Sr}, \text{Yb}, \text{Eu}$  and  $\text{T} =$  early transition metals from groups 4–7). Work is in progress to explore the contributing factors to the filling of the stuffed site and the ordering of the split site to form a potential supercell.

**Acknowledgment.** Financial support from the Department of Energy (Grant DE-FG02-99ER45793) is gratefully acknowledged. This work made use of the SEM facilities of the Center for Electron Optics at MSU. M.G.K. thanks the Guggenheim Foundation for a Fellowship.

**Supporting Information Available:** Synthetic procedures and characterization methods; crystallographic data (atomic positions, thermal parameters, bond lengths) for all compounds in the form of CIF files. This material is available free of charge via the Internet at <http://pubs.acs.org>.

IC034967Q

(11) Grin, Y. N.; Hiebl, K.; Rogl, P.; Godart, C.; Alleno, E. *J. Alloys Cmpd.* **1997**, *252*, 88–92.

(12) Reactions with Ca metal showed signs of attack of the quartz tube by Ca vapor; this was not apparent in reactions with perovskite  $\text{CaTiO}_3$ . This suggests that while the aluminum flux reduces the titanate species to  $\text{Ti}^0$ , the alkaline earth remains in its divalent state throughout the reaction.